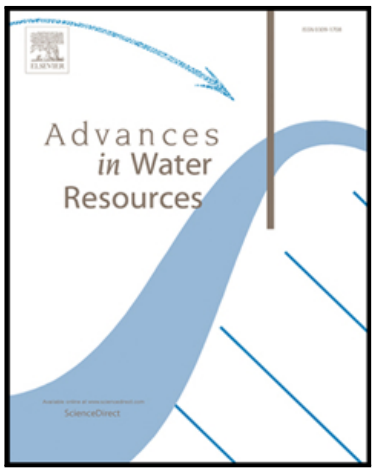

Catchment compatibility via copulas: a non-parametric study of the dependence structures of hydrological responses

S. Grimaldi, A. Petroselli, G. Salvadori, C. De Michele

PII: S0309-1708(16)30015-X
DOI: 10.1016/j.advwatres.2016.02.003
Reference: ADWR 2553

To appear in: *Advances in Water Resources*

Received date: 22 October 2015
Revised date: 1 February 2016
Accepted date: 4 February 2016

Please cite this article as: S. Grimaldi, A. Petroselli, G. Salvadori, C. De Michele, Catchment compatibility via copulas: a non-parametric study of the dependence structures of hydrological responses, *Advances in Water Resources* (2016), doi: 10.1016/j.advwatres.2016.02.003

Highlights

- dependence structures as signature of hydrological responses
- compatible catchments have similar dependence structures
- it is possibile to merge observed data for improving copula estimation in compatible catchments

Catchment compatibility via copulas: a non-parametric study of the dependence structures of hydrological responses

S. Grimaldi[a,1,*], A. Petroselli[b], G. Salvadori[c,2], C. De Michele[d]

[a]*DIBAF Department, University of Tuscia*
Via San Camillo de Lellis SNC, I-01100 Viterbo (Italy).
[b]*DAFNE Department, University of Tuscia*
Via San Camillo de Lellis SNC, I-01100 Viterbo (Italy).
[c]*Dipartimento di Matematica e Fisica, Università del Salento*
Provinciale Lecce-Arnesano, P.O.Box 193, I-73100 Lecce (Italy)
[d]*Department of Civil and Environmental Engineering, Politecnico di Milano*
Piazza Leonardo da Vinci 32, I-20133 Milano (Italy)

Abstract

The similarity of catchment responses is a fundamental issue for regionalization studies, and hydrograph attributes (i.e., Discharge Peak, Volume, and Duration) can reveal the signature and the synthesis of local scale processes. Here, we focus the attention on the "compatibility" between catchments, viz. on the possibility

*Corresponding author. Phone: +39-0761-357326; Fax: +39-0761-357356.
Email addresses: salvatore.grimaldi@unitus.it (S. Grimaldi), petro@unitus.it (A. Petroselli), gianfausto.salvadori@unisalento.it (G. Salvadori), carlo.demichele@polimi.it (C. De Michele)

[1]The support of the CRM-CANSSI (Université de Montréal, Montréal (Québec), Canada), where the work originated, is gratefully acknowledged.

[2]Helpful discussions with C. Sempi (Università del Salento, Italy), F. Durante (Free University of Bozen-Bolzano, Italy), I. Kojadinovic (Université de Pau et des Pays de l'Adour, France), and C. Genest (McGill University, Montréal (Québec), Canada) are acknowledged. The support of the CRM-CANSSI (Université de Montréal, Montréal (Québec), Canada), where the work originated, is gratefully acknowledged. The support of the CMCC (Centro Euro-Mediterraneo sui Cambiamenti Climatici, Lecce (Italy)) is acknowledged.

to transfer, from one catchment to another, the information about the dependence structures at play. In particular, we statistically investigate the possible relationships between the features of different Basin Scenarios (characterized via the Concentration Time T_c and the Curve Number CN) and the corresponding dependence structures ruling the joint statistics of Discharge, Volume, and Duration. Given a large set of synthetic runoff time series, generated via a rainfall-runoff model, recent non-parametric tests, based on empirical copulas, are used to compare the dependence structures associated with different soil uses and concentration times. The results indicate how the hydrological properties may affect the dependence structure. The outcomes of the investigation could be particularly effective in two practical applications: (1) for determining the degree of compatibility of the dependence structures associated with different basin scenarios, and (2) for enriching scanty data bases, in order to improve the estimation of multivariate copulas.

Keywords: Copula, Catchment compatibility, Rainfall-runoff transformation, Non-parametric test

1. Introduction

The concept of "hydrologic similarity", or "catchment similarity", stems from the idea that, despite the complexity of catchment response due to heterogeneities and different mechanisms involved, it exists a certain level of organization and

predictability of the catchment behavior. This concept allows to transfer the information from gauged to ungauged basins, and infer the hydrologic behavior in basins where no measurements are available (a common situation in hydrological practice).

The identification of hydrologic similarity requires a catchment classification (McDonnell and Woods, 2004), and consequently a catchment pooling, i.e. grouping basins which are considered hydrologically similar: this operation is not an easy task (Ali et al., 2012). In some cases, it results in a geographic region (also known as homogeneous region), in others in a cluster of basins (also known as region of influence), which has not necessarily the spatial contiguity, and may raise problems of spatial extrapolation when a leopard skin spatial distribution is obtained (Merz and Blöschl, 2005).

In literature, the hydrologic similarity has been considered to gain insights into the processes of runoff generation (see, e.g., Beven et al. (1988); Larsen et al. (1994); Blöschl and Sivapalan (1995); Robinson and Sivapalan (1997)), and to group together catchments for regional flood frequency analysis, and low-flow regionalization techniques (Laaha and Blöschl, 2006a).

In the last decades, several techniques have been developed to provide a catchment classification and investigate the hydrologic similarity. Some of these are

based on statistical simple or multiple scaling (Gupta and Waymire, 1990; Gupta and Dawdy, 1995; Gupta et al., 1994; Robinson and Sivapalan, 1997; De Michele and Rosso, 2002). Others have used the seasonality of discharges, through indices like Pardé or Burn ones (Pardé, 1947; Burn, 1990, 1997; Merz et al., 1999), or introducing a seasonality histogram (Laaha and Blöschl, 2006b), or metrics based on the mean seasonal water balance (Coopersmith et al., 2012; Ye et al., 2012; Petersen et al., 2012; Berghuijs et al., 2014). Other works have adopted cluster analysis techniques, like agglomerative hierarchical clustering, k-means clustering, and fuzzy partition clustering (Sawicz et al., 2011). Lastly, other approaches have adopted a combination of some of the above mentioned criteria (De Michele and Rosso, 2002). Despite the huge efforts devoted to the investigations of hydrologic similarity and catchment classification, and the results obtained, the uncertainty associated with the results requires further analyses.

The dependence structure among hydrological variables has recently become an intensively investigated topic for its pivotal implications in practical applications (Salvadori et al., 2007). The increasing interest, confirmed by a growing number of papers published on this issue (see `www.stahy.org` for a list of papers produced in the last ten years), is mainly due to the introduction of copulas and related tools (Sklar, 1959; De Michele and Salvadori, 2003). Indeed, the opportu-

nities offered by copulas have attracted many researchers on multivariate analysis that, nowadays, are transposing several traditional univariate hydrological studies into a multivariate perspective. In particular, according to the statement reported in the Directive 2007/60/EC of The European Parliament and of The Council (The European Parliament and The Council (6.11.2007)), a multivariate approach involving a number of non-independent variables should be considered for assessing the threatening of the phenomenon under investigation (The European Parliament and The Council, 6.11.2007, p. 31, Chapter III, Article 6.4).

In the last decade, several authors focused their attention on multivariate frequency analysis of hydrological variables, with the aim either to characterize their dependence structures (Salvadori and De Michele, 2004; Favre et al., 2004; Renard and Lang, 2007; Shiau et al., 2007; De Michele et al., 2007; Salvadori and De Michele, 2010, 2011; Haslauer et al., 2012; Salvadori et al., 2013; Louie, 2014), or to provide new insights for estimating multivariate design quantiles (Salvadori et al., 2011; De Michele et al., 2013; Gräler et al., 2013; Volpi and Fiori, 2014; Salvadori et al., 2015; Salvadori and De Michele, 2015). Moreover, a significant effort was devoted to include multivariate distributions in theoretical schemes for improving the performance of hydrological models (De Michele and Salvadori, 2003; Salvadori and De Michele, 2006; De Michele et al., 2007; Gao et al., 2007;

Bárdossy and Pegram, 2013; Motamedi and Liang, 2014; Hao and Aghakouchak, 2014).

Recently, the interest is spanning on new frontiers assuming that the dependence structure intrinsically contains a paramount of information about the dynamics of hydrological processes. For instance, multivariate trend analyses were applied (Ben Aissia et al., 2014; Huang et al., 2014; Chebana et al., 2013; Bender et al., 2014) assuming that the dependence structure could vary in time (and/or in space), enhancing the interpretation of its variability with respect to the classical univariate trend analysis. Interesting studies were also proposed concerning the use of copulas for evaluating the performance of hydrological models by comparing the dependence structure of simulated variables (Vandenberghe et al., 2011; Pham et al., 2013).

Particularly attractive is also the regional analysis of flood properties offered by Gaál et al. (2015), where the idea to relate the dependence structure of flood Discharge and Volume to the watershed physical properties is proposed. These authors illustrate an application to 330 catchments in Austria, characterized by different dimensions, climatic forcings, altitude, and presence of snow: although affected by relevant uncertainty due to the sample dimension and the strong heterogeneity of the hydrological and physical conditions, the results are encourag-

ing. Samaniego et al. (2010) proposed a measure of dissimilarity between basins based on the pairwise comparison of the empirical copula densities of runoff, and applied this to 38 German basins. Further contributions are available, with the aim to generalize the univariate regional procedure to a multivariate context (see, e.g., Salvadori and De Michele (2010); De Michele et al. (2013); Salvadori and De Michele (2015)).

The concept of "hydrologic similarity" is a notion featuring many facets, that leaves the door open to several possible definitions: in fact, the literature reports a number of approaches, based on different indices and techniques (Ali et al., 2012). This is probably due to the complexity of the problem, and to the fact that different indices account for distinct aspects of hydrologic similarity. Here, we focus the attention on a specific, yet unexplored, facet of the problem we name "catchment compatibility", which refers to the possibility of transferring, from one catchment to another, the information about the dependence structures at play, i.e. those ruling the joint behavior of the relevant variables. In particular, we statistically investigate the possible relationships between the features of Basin Scenarios (characterized by the Concentration Time T_c and the Curve Number CN) and the ones of the corresponding dependence structures regulating the joint statistics of Discharge, Volume, and Duration.

Long synthetic runoff time series are generated via a rainfall-runoff model, in order to make available large samples of hydrograph attributes related to specific basin scenarios, for different soil uses and concentration times. Recent non-parametric tests, based on empirical copulas, are used to compare the dependence structures associated with each basin scenario. Moreover, several strategies of comparison, either individual or ensemble, are proposed adopting statistical distances and equality tests between copulas. Among others, practical benefits consist in a valuable support to decide whether, and to what extent, time series collected in a basin characterized by a given pair (T_c, CN) could be used in order to improve the (statistical) knowledge of the copulas at play in another (partially or totally) ungauged basin with different T_c-CN features. Actually, since a crucial drawback in copula applications is often represented by the size of the available samples, we introduce, and test, a procedure to merge multivariate data sets collected in "compatible" basins, in order to improve the copula inference.

2. Materials

In this Section, details concerning the catchment case study, the framework for generating runoff time series, and the simulation experiment are provided.

2.1. The case study

The selected catchment is the Torbido river basin, located in central Italy. Torbido river is a small tributary of the Tiber, and is characterized by a drainage area of 61.67 km^2, elevations ranging from 85 to 625 m a.s.l., an average watershed slope of 21.9%, and a maximum distance between divide and outlet of 25.81 km. The Italian Geographic Military Institute provided the DEM with integer precision and a 20-m resolution (Italian Geographic Military Institute (IGMI), 2003), while land cover was retrieved from the website CORINE (European Environmental Agency (EEA), Programme of the European Commission, 2000): Table 1 summarizes the main features of the Torbido catchment.

Observed rainfall data are available from the Viterbo rain gauge station, located 30 km from the catchment centroid, for a period of 61 years (from 1951 to 1983, and from 1987 to 2014) at a daily time scale, and for a period of 10 years (from 2005 to 2014) at a 1-hour resolution.

2.2. The hydrologic model

The adopted hydrological model is the recently developed simulation framework named COSMO4SUB (COntinuous Simulation MOdel For Small Ungauged Basins — see Grimaldi et al. (2012b,c)). COSMO4SUB consists in a multi-step procedure characterized by a rainfall generator, an infiltration model, and

a rainfall-runoff model.

Regarding the first step, the HyetosR 1.1 software was used (see Koutsoyiannis and Onof (2001), and `www.itia.ntua.gr/en/softinfo/3/`). HyetosR is a package for the temporal stochastic simulation of rainfall process at fine time scales (say, less than one day) that uses (1) the Bartlett-Lewis rectangular pulses rainfall model (Onof and Wheater, 1993, 1994), and (2) suitable disaggregation techniques (Koutsoyiannis, 2001) that adjust the finer scale values in order to obtain the required coarser scale values without affecting the stochastic structure of the data. The model was calibrated on the observed rainfall data.

Regarding the second step, the Soil Conservation Service-Curve Number (SCS-CN) method (USDA-SCS, 1986) was used in order to calculate the rainfall excess. The SCS-CN method was applied assigning the value 0.2 to the parameter involved in the calculation of initial abstraction, as suggested in the official formulation (USDA-NRCS, 2010).

Regarding the third step, a geomorphological rainfall-runoff model was applied to the excess rainfall time series estimated in the previous step, in order to obtain the corresponding runoff time series. An advanced version of the well-known Width Function Instantaneous Unit Hydrograph (WFIUH) was employed (Grimaldi et al., 2012a), viz. the so called WFIUH-1par, which can be calibrated

fixing only one parameter related to the value of the concentration time T_c.

Finally, flood hydrographs are selected as sequences of positive runoff values separated by at least one zero value. The two main parameters of the COSMO4SUB framework are CN and T_c. The former parameter controls all the processes causing rainfall losses (infiltration, evapotranspiration, etc.), and is mainly related to the soil use and type. Increasing the CN value, a growth of rainfall excess total amount, of rainfall excess maximum intensity, and consequently of durations, are expected. In turn, all the hydrograph attributes are expected to get larger by increasing the parameter CN. Instead, T_c corresponds to the IUH base time, so it is representative of the catchment runoff velocity. For large T_c's, small hydrograph peak discharges and long duration are expected. From a physical perspective, this parameter is mainly related to the soil use, slopes, and drainage network structure.

2.3. The simulation procedure

The simulation procedure adopted in this work generates long synthetic runoff time series associated with specific parameters responsible of the runoff generation. The plan of action is based on the following steps.

1. Given a small catchment (described in Section 2.1), the COSMO4SUB model is applied as described in Section 2.2: in turn, runoff time series at 1-hour resolution and 500 years long are generated.

2. Varying the parameter CN from 50 to 100 (with a step of $\Delta_{CN} = 5$) and the parameter T_c from 4 to 13 hours (with a step of $\Delta_{T_c} = 1$ hour), a set of 110 different combinations were considered: hereinafter, each pair (T_c, CN) will be referred to as a Basin Scenario (BS). Practically, the catchment conditions range from

   - a "minimal" combination (13h and 50), for which it is expected a strong filtering of rainfall input due to the rainfall-runoff transformation, up to
   - a "maximal" combination (4h and 100), representing a fully urbanized catchment.

   In addition, in order to perform a statistically consistent analysis of the uncertainty inherent the random simulations, a set of $N_S = 100$ independent rainfall time series was generated for each of the 110 BS's: thus, a total of 11,000 data bases are made available.

3. Selecting the maximum annual flood Discharge values, and the related hydrograph Volume and Duration, a set of 500 simulated triples Discharge-Volume-Duration are extracted from each of the 11,000 rainfall-runoff series.

Then, several valuable statistical analyses and comparisons can be carried out (see Section 3): viz., the calculation of the degree of association between the relevant variables, the comparison of the Empirical Copulas (*EC*) of interest, the estimate of suitable statistical distances between the dependence structures at play, and the test of equality of the copulas associated with different BS's.

It is worth stressing that, at present, only in a few elementary cases, it is possible to guess what should be the features of the copula describing the dependence structure of data generated by a given model: evidently, this is not the case of the involved simulation framework used in this work. Concerning the analysis of the results, the problem can be bypassed by adopting a non-parametric approach, as shown below. Instead, understanding how the model structure/parameterization may affect the copulas of interest is still an open issue, especially when the model is a complex one.

3. Methods and results

As mentioned in the Introduction, the target of this work is to investigate the possible relationships between different Basin Scenarios — as identified by the parameters (T_c, CN) — and the corresponding structures of dependence (viz., the 2-copulas) associated with three relevant pairs of variables: namely, the Discharge-

Volume, the Discharge-Duration, and the Volume-Duration.

As a fundamental point, all the analyses carried out in the sequel are non-parametric: i.e., no parametric models (univariate and/or multivariate) are fitted to the available data. In particular, all the statistical tests are non-parametric, essentially based on the calculation/comparison of the Empirical Copulas of interest. In fact, the use of a parametric approach would involve the selection of specific probability laws, entailing the introduction of unnecessary arbitrariness: in turn, the results would depend upon the choices of the distributions, a nuisance that can be bypassed adopting proper non-parametric techniques, as done in this work. Apparently, the non-parametric tests mentioned below are robust against small sample sizes, e.g. in case short time series were available (say, 20–30 years).

It is worth stressing that many of the statistical analyses presented in later Sections assume that the samples investigated consist of independent identically distributed vectors. Here the independence assumption may be taken for granted, both for physical and statistical reasons, since the triples in the series correspond to maximum annual flood events. Instead, changes of the probability distributions at play need to be specifically investigated. For this reason, recent non-parametric univariate/multivariate tests for change point detection (Holmes et al., 2013; Kojadinovic, 2014) are used to check whether the series could be considered as "sta-

tionary" or not. In particular, for each of the 110 BS's (T_c, CN)'s examined here, all the pairs Discharge-Volume, Discharge-Duration, and Volume-Duration, and all the triples Discharge-Volume-Duration corresponding the N_S independent series are checked out (for a total of 44,000 tests). The results (not shown for the sake of brevity) suggest that the dependence structures of interest could empirically be assumed as "stationary", since possible change points are statistically detected in less than 5% of the cases (at a standard 5% level), for all the BS's and variables.

3.1. Measuring the degree of association

The use of multivariate dependence structures for modeling the variables at play only makes sense when these variables are non-independent. As a first preliminary (but necessary) analysis, two standard measures of association, i.e. the Kendall τ and the Spearman ρ coefficients (Nelsen, 2006; Salvadori et al., 2007), are computed for the three pairs Discharge-Volume, Discharge-Duration, and Volume-Duration, considering all the 110 BS's of interest here. In particular, for each pair (T_c, CN), both τ and ρ are independently estimated N_S times using all the available series for each BS. The corresponding sample averages and standard deviations are then considered, as well as the p-Values of the related non-parametric Kendall and Spearman tests of independence.

Here, only the outcomes concerning the Kendall τ are presented, since the ones involving the Spearman ρ are analogous. Figures 1 show the sample averages of τ, over all the available N_S series, and the corresponding sample standard deviations, for all the BS's and the three pairs Discharge-Volume, Discharge-Duration, and Volume-Duration.

In all cases, the estimated Kendall τ's are positive, and significantly different from zero, as suggested by the negligible p-Values of the corresponding independence tests. In turn, all the three pairs of variables are concordant, and cannot be statistically independent. It is worth noting that, apparently, the estimates are well centered around the corresponding mean values, since the variances are very small. A first analysis of the results suggests the following considerations.

1. The parameter τ changes by varying CN, whereas it is roughly constant by varying T_c.
2. In general, on the T_c–CN grid, adjacent BS's are associated with close values of τ, viz. the parameter shows a slow variation over the grid.
3. In the Volume-Duration case, the parameter τ is roughly constant over all the T_c–CN grid, whereas a significant variability is present in the Discharge-Volume and Discharge-Duration cases.
4. The parameter τ decreases by increasing CN in the Discharge-Volume and

Discharge-Duration cases. Physically, for low values of CN, relevant losses are expected, thus reducing the variety of net rainfall events: most of the net hyetographs are concentrated in one-time steps, generating a strong dependence between Discharge-Volume (and Discharge-Duration) hydrographs. On the contrary, increasing the CN, the net rainfall events will be similar to the gross rainfall, preserving a complex time structure and, consequently, providing a larger range of volumes (and durations) for a specific Discharge.

5. As expected, Discharge-Volume pairs are characterized by the largest values of τ, whereas the lowest degrees of association are present in Discharge-Duration case. The physical reason is due to the rainfall variability and the hyetograph structure. While a flood event with a significant peak will most likely be associated with a large volume (due to the recession curve of the hydrograph), not necessarily a large duration yields a high peak discharge. Indeed, it is possible to have a rainfall event characterized by low intensity values and a long duration that generates a low peak discharge with long duration.

6. Concerning the Discharge-Volume case, the results are consistent with those shown in Gaál et al. (2015, Figure 5). Indeed, in the present case study (involving a basin of about 62 Km^2), τ approximately ranges in the interval

0.6–0.9, essentially the same one reported in the cited paper for a basin of similar dimension.

As a conclusion, the results outlined above legitimate the use of a multivariate approach, as done in the present work.

3.2. Comparing copulas for different BS's

A preliminary rough examination of the similarity/dissimilarity of the dependence structures associated with different BS's consists in a visual comparison of the EC's estimated for several combinations of the parameters (T_c, CN)'s. The procedure is as follows.

1. Three values of T_c are selected (viz., $T_c = 240, 480, 780$ minutes), ranging from the minimum available T_c to the maximum one. Similarly, a triple of CN's (viz., $CN = 50, 75, 100$) is selected, covering the range of investigated values.
2. The EC's of the pairs Discharge-Volume, Discharge-Duration, and Volume-Duration are estimated by fixing the value of T_c (or CN), and leaving the other variable vary in the corresponding subset. The EC's are evaluated over a fine 65×65 uniform grid $\mathcal{G}$ on the unit square $\mathbf{S}$ (with a linear resolution equal to $1/64$) — clearly, different grids could be used: thus, a total of

$N_G = 65^2 = 4225$ sampling points are considered. Since N_S independent series are available for each BS, then the grid averages of the EC's (over the N_S series) are used as reference values: these provide consistent non-parametric estimates of the copulas of interest at each point of the grid $\mathcal{G}$.

3. The contours (isolines) of the average EC's are then plotted on the same graphs for selected probability levels: here, $0.1, 0.3, 0.5, 0.7, 0.9$. Different plots can thus be compared.

The visual comparison of the (average) EC's estimated for several combinations of the parameters (T_c, CN)'s is shown in Figures 2 and 3, for fixed T_c's and CN's, respectively, and the three pairs Discharge-Volume, Discharge-Duration, and Volume-Duration. Some preliminary comments are as follows.

Apparently, in general the role played by the parameter T_c looks marginal, at least considering the pairs Discharge-Volume and Discharge-Duration. In fact, analyzing Figure 2 column-wise, the three plots in the same column are quite similar, and little changes by increasing the parameter T_c from top to bottom. Actually, as shown in Figure 3 (where CN is fixed), the isolines corresponding to the three T_c values are over-lapping, or just barely different.

Furthermore, consider the pair Discharge-Volume, and the smallest value of the parameter CN (viz., 50), as plotted in Figures 2(left column) and 3(top-left).

Apparently, the structure of the corresponding (average) 2-copula is similar to the one of the co-monotone 2-copula $\mathbf{M}_2(u, v) = \min(u, v)$ — see, e.g., Salvadori et al. (2007, Figure 3.4) — describing the dependence structure of variables functionally positively associated. As before (see the comments in Section 3.1 concerning the Kendall τ), for low values of CN almost all of the rainfall amount infiltrates, and the net rainfall is often represented by a single time step, thus yielding a functional dependence between Discharge and Volume hydrographs.

3.3. Distance and equality of copulas

In order to investigate the "closeness" of the dependence structures associated with different Basin Scenarios, we use two suitable statistical tools: namely, a *distance*, and an *equality test*, as discussed below. In the present context, the adjective "statistical" is mandatory, since the copulas of interest are estimated via random samples. A positive distance between copulas is a necessary condition in order to assess the non-equality of copulas. However, it is not a sufficient one: as will be shown later, two copulas may be statistically equal, even if their distance is positive. The explanation of such a counter-intuitive fact is that, here, the notions of distance and equality are taken in a statistical sense, in order to correctly cope with the randomness of the phenomena investigated. Roughly speaking, "small" distances can be (statistically) compatible with the equality of copulas.

In order to quantify how distant two dependence structures are (according to a specific metrics), among many possible choices — see, e.g., Genest et al. (2009) — the L^2 norm and the L^∞ (or sup) norm criteria are frequently used in applications. The former one corresponds to a Cramér-von Mises (CvM) approach, while the latter one is based on statistics of Kolmogorov-Smirnov (KS) type. We anticipate here that, for the sake of brevity, only the results concerning the CvM option will be illustrated in the sequel, the KS case yielding analogous outcomes.

Let $\mathbf{C}_1$ and $\mathbf{C}_2$ be the copulas associated with, respectively, the BS's $\mathcal{S}_1 = (T_{c,1}, CN_1)$ and $\mathcal{S}_2 = (T_{c,2}, CN_2)$, and denote by $\delta_{1,2}$ the distance between $\mathbf{C}_1$ and $\mathbf{C}_2$. Then, in the CvM case, the following definition may be introduced:

$$\delta_{1,2} = 24 \cdot \int_{\mathbf{u}\in\mathbf{S}} (\mathbf{C}_1(\mathbf{u}) - \mathbf{C}_2(\mathbf{u}))^2 \, d\mathbf{u}, \tag{1}$$

where the coefficient "24" is used to normalize δ into the interval $[0, 1]$ (Nelsen, 2006). A consistent empirical estimator $\widetilde{\delta}_{1,2}$ of $\delta_{1,2}$ is given by

$$\widetilde{\delta}_{1,2} = 24 \cdot \sum_{\mathbf{u}\in\mathcal{G}} \left(\widetilde{\mathbf{C}}_1(\mathbf{u}) - \widetilde{\mathbf{C}}_2(\mathbf{u})\right)^2 / N_G, \tag{2}$$

where $\widetilde{\mathbf{C}}_\bullet$ denotes the EC corresponding to the copula $\mathbf{C}_\bullet$. For the sake of completeness, the KS case is outlined in Appendix B.

Practically, the estimation of $\delta_{1,2}$ is carried out as follows.

1. Two different BS's $\mathcal{S}_1$ and $\mathcal{S}_2$ are selected, and the EC's of the three pairs

Discharge-Volume, Discharge-Duration, and Volume-Duration are estimated for both $\mathcal{S}_1$ and $\mathcal{S}_2$ over the grid $\mathcal{G}$.

2. Since N_s independent series are available for each BS, then N_s values of $\widetilde{\delta}_{1,2}$ can be calculated, using either Eq. (2) or Eq. (B.2): clearly, such a sample can be used to extract valuable empirical information about the distribution of $\delta_{1,2}$. For instance, the sample mean (or median) may provide indications about the central value of the distance, the sample standard deviation may supply information about its variability, and suitable non-parametric empirical Confidence Intervals may be calculated as well, by properly using the associated Order Statistics.

It is worth pointing out that, per se, the notion of distance has only a relative meaning, and should only be used for doing relative comparisons: roughly speaking, larger distances in general correspond to more dissimilar copulas.

In fact, the crucial question whether two copulas are equal or not can only be answered via a suitable statistical test. A non-parametric procedure for testing the equality between copulas has recently been outlined in Rémillard and Scaillet (2009); Rémillard and Plante (2012): the test indicates whether the null hypothesis $\mathcal{H}_0$ that two copulas are the same should be statistically rejected or not. In the present context, the test is used to compare copulas associated with pairs of vari-

ables simulated under different Basin Scenarios: clearly, if $\mathcal{H}_0$ cannot be statistically rejected, then presumably the data share a common dependence structure. Here, given two different BS's $\mathcal{S}_1$ and $\mathcal{S}_2$, the N_S copulas of the pairs Discharge-Volume, Discharge-Duration, and Volume-Duration are compared at a standard 5% level. In turn, the percentage of non-rejection of $\mathcal{H}_0$ (over the N_S tests) may provide valuable empirical information about the similarity of the copulas of interest: clearly, large percentages of non-rejection may support the statistical equality of the copulas considered.

3.4. Investigating the compatibility of BS's

As mentioned above, a Basin Scenario is characterized via the corresponding pair (T_c, CN), i.e. a two-parameter identification: Figure 4(top-left) illustrates the T_c–CN grid considered here, consisting of 110 different BS's. Note that, one step in the CN direction corresponds to a jump of size $\Delta_{CN} = 5$, while one step in the T_c direction corresponds to a jump of size $\Delta_{T_c} = 60$ minutes. For instance, the two BS's X and Y plotted in the picture are 7 units far apart in the CN direction, and 5 units far apart in the T_c direction: evidently, X and Y correspond to (very) dissimilar hydrological scenarios.

In this work, we are interested in understanding whether, and how, the parameters T_c and CN may affect the dependence structures of the data bases simulated

according to different (T_c, CN) settings. The methodology outlined in this Section represents a preliminary necessary step in order to assess under which conditions *data sets generated according to different BS paradigms could be interchanged* (viz., are "compatible"), when the interest is in the dependence structures at play.

In order to investigate the compatibility of different Basin Scenarios, we introduce here several concepts, exploiting the statistical tools outlined in the previous Section. In particular, general definitions of BS compatibility are proposed, based either on an "individual" or an "ensemble" rationale involving the dependence structures of interest. In the former case, the copula corresponding to a reference BS X is compared with the one associated with a single neighbor BS Y (viz., only two BS's at a time are involved). In the latter case, the copula corresponding to a reference BS X is compared with a family of copulas associated with a set of neighboring BS's Y's (viz., a number of different BS's is considered at a time).

Here, three different approaches are outlined: all the notions are based on the test of equality mentioned in Section 3.3, as well as on the distance δ. Actually, three further strategies can be considered: these are briefly introduced in Appendix A, and illustrated in Figure 4; however, for the sake of brevity, they will not be discussed in this work.

Pairwise. Consider two generic BS's X and Y, such as those illustrated in Figure

4(top-left). Their Pairwise BS (individual) distance is defined as the average δ distance (over the N_s series) between them. Correspondingly, the Pairwise BS (individual) compatibility between X and Y is defined as the percentage of equality tests (over the N_s series) for which the assumption $\mathcal{H}_0$ should not be rejected.

Foreword-CN (fCN). The fCN BS (individual) distance of size d is defined as the average δ distance (over the N_s series) between the BS's $\mathcal{S}_1 = (T_c, CN)$ and $\mathcal{S}_2 = (T_c, CN + d \cdot \Delta_{CN})$. The notion is illustrated in Figure 4(bottom-right), using d's ranging from 1 to 4. Correspondingly, their fCN BS (individual) compatibility is defined as the percentage of equality tests (over the N_s series) for which the assumption $\mathcal{H}_0$ should not be rejected. Clearly, the fCN approach is a special case of the Pairwise one: here, the parameter T_c is kept fixed.

Ring. The Ring BS (ensemble) distance of size d is defined as the average (over the N_s series) of the average δ distance between the BS $\mathcal{S} = (T_c, CN)$ and all the neighboring BS's lying on a suitable "d-ring" surrounding $\mathcal{S}$ on the T_c–CN grid: viz., at least one of the neighbor parameters T_c or CN is equal to $T_c \pm d \cdot \Delta_{T_c}$ or $CN \pm d \cdot \Delta_{CN}$. The notion is illustrated in Figure 4(top-right), for

d equal to 1 and 2. Practically, the Ring distance is the average of all the BS distances considering the neighbors of $\mathcal{S}$ positioned on a suitable frame surrounding $\mathcal{S}$ on the T_c–CN grid. Note that the Ring approach averages over "full" changes of the basin parameters, and may provide an overall picture of the differences between the BS $\mathcal{S}$ and its neighbors. Correspondingly, the Ring BS (ensemble) compatibility is defined as the average percentage of equality tests (over the N_s series) for which the assumption $\mathcal{H}_0$ should not be rejected, when testing the equality between $\mathcal{S}$ and all its Ring neighbors.

Clearly, BS distances and compatibilities can be computed by considering only the neighboring BS's inside the T_c–CN grid: in fact, for large d's, some of the surrounding BS's may not lie inside the T_c–CN grid, and would not be admissible. From a statistical point of view, this means that some averages are calculated using different sample sizes, but such a nuisance is geometrically unavoidable.

As an illustration of the Pairwise approach, consider the three BS's labelled X, Y, and Z in Figure 4(top-left). The sample averages and standard deviations (over the N_S series) of the distance δ between the pairs {X,Y}, {X,Z}, and {Y,Z} are reported in Table 2, considering the variables Discharge-Volume, Discharge-Duration, and Volume-Duration. It is interesting to note that, in general, the values of δ for the pair {X,Y} are larger than the corresponding ones for the pairs {X,Z}

and {Y,Z}.

The results concerning the fCN and the Ring strategies are illustrated in Figures 5–6 for $d = 1$, and in Figures 7–8 for $d = 2$, and are commented below.

The case $d = 1$. Both the fCN and the Ring average distances look rather small and homogenous over all the T_c–CN grid, and the very small standard deviations indicate the presence of negligible fluctuations, for all the BS's considered.

The case $d = 2$. As a difference with the previous case, both the fCN and the Ring average distances get larger, and also more heterogeneously distributed over the T_c–CN grid. In general, also the standard deviations slightly increase, indicating a greater variability.

The results presented above are not surprising: in fact, larger d's are expected to yield more distant BS's under the fCN and Ring approaches.

3.5. Compatibility Maps

As mentioned above, the percentage of non-rejection of $\mathcal{H}_0$ may provide an empirical tool to evaluate the similarity of the copulas corresponding to different BS's. A comparison procedure can be put at work by introducing the so-called

Compatibility Maps (*CM*). In the present context, the resolution of the maps is $\Delta_{CN} = 5$ in the *CN* direction, and $\Delta_{T_c} = 60$ minutes in the T_c direction.

The procedure is as follows: for the sake of brevity, only the Pairwise case is considered here, the others being analogous. Firstly, a BS $\mathcal{S}$ is selected, and the Pairwise compatibility of $\mathcal{S}$ with respect to all the remaining BS's is computed: in the present setting, there are 109 possible neighbors. Secondly, the plot on the T_c–*CN* grid of the non-rejection percentages of $\mathcal{H}_0$ provides a Pairwise CM for the BS $\mathcal{S}$. In turn, the data collected under BS's whose percentage of non-rejection is large enough (say, larger than 90%, or 95%, or any other suitable threshold) could be labelled as "compatible" with the observations in $\mathcal{S}$.

As an illustration, here the three BS's labelled X, Y, and Z in Figure 4(top-left) are assumed to characterize the basins of reference: the target is to spot which are the BS's "compatible" with the reference ones, by constructing the corresponding CM's, and identifying possibly admissible neighboring BS's. The results are shown in Figure 9. The situation varies by considering different pairs of variables (viz., either the Discharge-Volume, or the Discharge-Duration, or the Volume-Duration ones), and the (T_c, CN) parameters associated with X, Y, or Z. Considering the Volume-Duration case, it is clear that at least all the BS's in a surrounding ring of size $d = 1$ would be admissible, being the percentages of non-

rejection close to 100%. Instead, in the Discharge-Duration case, only some of the BS's in a surrounding ring of size $d = 1$ would be fully admissible, although the percentages of non-rejection are large for all the eight neighbors of the reference BS's. Finally, in the Discharge-Volume case, the BS X turns out to be compatible with a surrounding ring of BS's of size $d = 2$ (and similarly for Z, considering a ring of size $d = 1$), whereas the BS Y seems to be compatible only with the closest BS's in the same column of the T_c–CN grid. Further examples of Compatibility Maps are shown in Figures 5–8, considering both the Foreword-CN and the Ring approaches, and grid distances of size $d = 1$ and $d = 2$.

3.6. Merging different data bases

As already mentioned above, often the size of a sample collected at a given site may be insufficient for statistical purposes: for instance, the estimate and validation of multivariate dependence structures may not be accurate by using inadequate data bases. In turn, the idea is to try and increase the actual sample size by "merging" the available data with other observations collected in "compatible" basins. For this purpose, the Compatibility Maps introduced in Section 3.5 could be used to understand and single out which external data bases might be appropriate to flesh out the scarce one.

As for the concepts of basin compatibility, also the merging task may be either

individual or ensemble: viz., the external data may be picked up from a single data base, or from a number of data bases. In the former case, the Pairwise (or fT_c, or fCN) procedure provides a natural selection criterion. In the latter case, a global survey can be carried out simultaneously over all the external data bases by using an ensemble criterion (e.g., the Ring, the Diagonal, or the Cross strategy): for instance, considering the Ring approach, the BS's of the data bases involved should belong to an admissible ring on the (T_c, CN)-grid, centered on the target BS $\mathcal{S}$.

A workable methodology for merging distinct data bases (possibly of different sizes) is as follows: the pseudo-observations (i.e., the ranks divided by the sample size — see, e.g., Genest and Favre (2007)) associated with the available data are first calculated, and then combined. In case ties (i.e., repeated values) were present, then suitable randomizations may be performed in order to remove them (Kojadinovic and Yan, 2010; Hofert et al., 2015). Note that all the standard non-parametric procedures for estimating copulas are based on the pseudo-observations.

A simple method to test whether the merging procedure outlined above makes sense is as follows. First, a series is split into two halves, and the pseudo-observations of each subset are computed, and subsequently combined. Then, the

EC associated with the merged data base is compared with the original one via an equality test, in order to statistically check whether the two are "compatibile": clearly, this represents a necessary condition for the validity of the merging operation. In the present study, such a test was carried out considering all the 110 BS's of the T_c–CN grid, and all the N_S series: as a result, only in a dozen out of the 33,000 equality tests the statistical hypothesis that the original and merged copulas were the same was rejected (at a 5% level).

A study of the performances of the merging techniques outlined above was carried out by considering the three BS's X, Y, and Z already investigated in Section 3.4 — see Figure 4(top-left). In particular, the Ring merging strategy was adopted, using $d = 1$ and $d = 2$. Tables 3 and 4 show, respectively, the corresponding percentages of non-rejection of $\mathcal{H}_0$: here the EC's of the simulated series are compared with those of the merged data bases of the admissible Ring neighbors. In addition, for the sake of visual comparison, Figures 10 and 11 show, respectively, the comparison between the EC's of the "true" and the "merged" series (averaged over the N_S series), for $d = 1$ and $d = 2$, considering the BS's X, Y, and Z, and the pairs Discharge-Volume, Discharge-Duration, and Volume-Duration.

As expected, in general the percentages of non-rejection of $\mathcal{H}_0$ decrease by

increasing the grid distance d: obviously, further neighbors ($d = 2$) are less compatible than closer ones ($d = 1$). It is interesting to note that, in the case $d = 1$, all the percentages are larger than 90%: this may indicate a significant compatibility between the series of the BS's X, Y, and Z, and those of the corresponding Ring neighbors. The analysis is visually confirmed by the plots shown in Figures 10 and 11: in fact, large percentages in Tables 3 and 4 are generally associated with almost overlapping isolines, whereas significant differences of the contour plots generally correspond to small percentages.

4. Conclusions

This paper investigates a specific, yet unexplored, aspect of hydrologic similarity, viz. the catchment compatibility with respect to the similarity of the copulas at play under different Basin Scenarios. In particular the possible relations between hydrological responses and corresponding dependence structures are analyzed by means of simulation tests, where relevant hydrological variables are generated in a small catchment under controlled conditions. For this purpose, a hydrological model is used, keeping constant both the climatic forcing (synthetic rainfall time series) and the topography, whereas the Curve Number and the Concentration Time are varied. Such a procedure provides a number of scenarios

(110, in the present study) that differ from one another only for the parameter responsible of the infiltration and losses processes, and the runoff velocity in the watershed. For each scenario, 500 years of runoff are simulated, and the triples of Discharge-Volume-Duration corresponding to maximum annual floods are selected.

Measures of association, empirical copula visual comparison, Cramér-von Mises distances between dependence structures, non-parametric procedures for testing the equality among bivariate copulas, and a variety of compatibility definitions (individual and/or ensemble) are applied on the pairs Discharge-Volume, Discharge-Duration, and Volume-Duration, yielding suitable Compatibility Maps. This latter tool provides an easy way to (statistically) evaluate which T_c-CN combinations may yield compatible dependence structures.

On the one hand, these preliminary results could pave the way for a possible new approach concerning the identification of "compatible" basins. On the other hand, given two (or more) "compatible" catchments, workable criteria and procedures have been stated for merging the available data: clearly, increasing the sample size may improve the estimation of the copulas at play, providing an useful tool for bypassing the lack of hydrological observation (a crucial problem in applications).

The results presented in this work suggest further investigations both on the relation between dependence structure and hydrological parameters, and on the practical implications of the approach proposed. Indeed, the next research step will involve a more complex model, as well as a wider range of climatic forcings, in order to achieve a thorough survey of the relations between dependence structure and physical attributes. In addition, a set of case studies (with limited observations) will be tested, in order to check the practical potentiality of the merging procedure and the compatibility maps.

References

Ali, G., Tetzlaff, D., Soulsby, C., McDonnell, J. J., Capell, R., 2012. A comparison of similarity indices for catchment classification using a cross-regional dataset. Advances in Water Resources 40 (0), 11–22.

Bárdossy, A., Pegram, G., 2013. Interpolation of precipitation under topographic influence at different time scales. Water Resources Research 49 (8), 4545–4565.

Ben Aissia, M.-A., Chebana, F., Ouarda, T., Roy, L., Bruneau, P., Barbet, M., 2014. Dependence evolution of hydrological characteristics, applied to floods in a climate change context in Quebec. Journal of Hydrology 519 (PA), 148–163.

600 Bender, J., Wahl, T., Jensen, J., 2014. Multivariate design in the presence of non-
601 stationarity. Journal of Hydrology 514, 123–130.

602 Berghuijs, W., Sivapalan, M., Woods, R., Savenije, H., 2014. Patterns of similarity
603 of seasonal water balances: A window into streamflow variability over a range
604 of time scales. Water Resources Research 50 (7), 5638–5661.

605 Beven, K., Wood, E., Sivapalan, M., 1988. On hydrological heterogeneity - catch-
606 ment morphology and catchment response. Journal of Hydrology 100 (1-3),
607 353–375.

608 Blöschl, G., Sivapalan, M., 1995. Scale issues in hydrological modelling: a re-
609 view. Hydrological Processes 9 (3-4), 251–290.

610 Burn, D., 1990. Evaluation of regional flood frequency analysis with a region of
611 influence approach. Water Resources Research 26 (10), 2257–2265.

612 Burn, D., 1997. Catchment similarity for regional flood frequency analysis using
613 seasonality measures. Journal of Hydrology 202 (1-4), 212–230.

614 Chebana, F., Ouarda, T., Duong, T., 2013. Testing for multivariate trends in hy-
615 drologic frequency analysis. Journal of Hydrology 486, 519–530.

616 Coopersmith, E., Yaeger, M., Ye, S., Cheng, L., Sivapalan, M., 2012. Exploring

the physical controls of regional patterns of flow duration curves - part 3: A catchment classification system based on regime curve indicators. Hydrology and Earth System Sciences 16 (11), 4467–4482.

De Michele, C., Rosso, R., 2002. A multi-level approach to flood frequency regionalisation. Hydrology and Earth System Sciences 6 (2), 185–194.

De Michele, C., Salvadori, G., 2003. A generalized pareto intensity-duration model of storm rainfall exploiting 2-copulas. J. Geophys. Res. 108 (D2), 4067.

De Michele, C., Salvadori, G., Passoni, G., Vezzoli, R., 2007. A multivariate model of sea storms using copulas. Coast. Eng. 54, 734–751.

De Michele, C., Salvadori, G., Vezzoli, R., Pecora, S., 2013. Multivariate assessment of droughts: frequency analysis and Dynamic Return Period. Water Resour. Res. 49 (10), 6985–6994.

European Environmental Agency (EEA), Programme of the European Commission, 2000. CORINE (Coordination of Information on Environment). Database, a key database for European integrated environmental assessment.

Favre, A.-C., El Adlouni, S., Perreault, L., Thiamonge, N., Bobee, B., 2004. Multivariate hydrological frequency analysis using copulas. Water Resour. Res. 40.

Gaál, L., Szolgay, J., Kohnová, S., Hlavčová, K., Parajka, J., Viglione, A., Merz, R., Blöschl, G., 2015. Dependence between flood peaks and volumes – a case study on climate and hydrological controls. Hydrological Sciences Journal 60 (6), 968–984.

Gao, H., Wood, E., Drusch, M., McCabe, M., 2007. Copula-derived observation operators for assimilating TMI and AMSR-E retrieved soil moisture into land surface models. Journal of Hydrometeorology 8 (3), 413–429.

Genest, C., Favre, A. C., 2007. Everything you always wanted to know about copula modeling but were afraid to ask. J. Hydrologic Engineering 12 (4), 347–368.

Genest, C., Rémillard, B., Beaudoin, D., 2009. Goodness-of-fit tests for copulas: A review and a power study. Insurance: Mathematics and Economics 44, 199–213.

Gräler, B., van den Berg, M. J., Vandenberghe, S., Petroselli, A., Grimaldi, S., Baets, B. D., Verhoest, N. E. C., 2013. Multivariate return periods in hydrology: a critical and practical review focusing on synthetic design hydrograph estimation. Hydrol. Earth Syst. Sci. 17, 1281–1296.

Grimaldi, S., Petroselli, A., Nardi, F., 2012a. A parsimonious geomorphological

652 unit hydrograph for rainfall-runoff modelling in small ungauged basins. Hydro-
653 logical Sciences Journal 57 (1), 73–83.

654 Grimaldi, S., Petroselli, A., Serinaldi, F., 2012b. A continuous simulation model
655 for design-hydrograph estimation in small and ungauged watersheds. Hydro-
656 logical Sciences Journal 57 (6), 1035–1051.

657 Grimaldi, S., Petroselli, A., Serinaldi, F., 2012c. Design hydrograph estimation in
658 small and ungauged watersheds: continuous simulation method versus event-
659 based approach. Hydrological Processes 26 (20), 3124–3134.

660 Gupta, V., Dawdy, D., 1995. Physical interpretations of regional variations in the
661 scaling exponents of flood quantiles. Hydrological Processes 9 (3-4), 347–361.

662 Gupta, V., Mesa, O., Dawdy, D., 1994. Multiscaling theory of flood peaks: re-
663 gional quantile analysis. Water Resources Research 30 (12), 3405–3421.

664 Gupta, V., Waymire, E., 1990. Multiscaling properties of spatial rainfall and river
665 flow distributions. Journal of Geophysical Research 95 (D3), 1999–2009.

666 Hao, Z., Aghakouchak, A., 2014. A nonparametric multivariate multi-index
667 drought monitoring framework. Journal of Hydrometeorology 15 (1), 89–101.

Haslauer, C., Guthke, P., Bárdossy, A., Sudicky, E., 2012. Effects of non-gaussian copula-based hydraulic conductivity fields on macrodispersion. Water Resources Research 48 (7).

Hofert, M., Kojadinovic, I., Maechler, M., Yan, J., March 2015. copula: Multivariate Dependence with Copulas. 0th Edition, http://cran.r-project.org/web/packages/copula.

Holmes, M., Kojadinovic, I., Quessy, J.-F., 2013. Nonparametric tests for change-point detection à la Gombay and Horváth. Journal of Multivariate Analysis 115, 16–32.

Huang, S., Chang, J., Huang, Q., Chen, Y., 2014. Identification of abrupt changes of the relationship between rainfall and runoff in the Wei River Basin, China. Theoretical and Applied Climatology(in press).

Italian Geographic Military Institute (IGMI), 2003. Raster (Matrix) numerical DEM of Italy. www.igmi.org/pdf/info_matrix2003.pdf, (internal factsheet; in Italian).

Kojadinovic, I., 2014. npcp: Some nonparametric tests for change-point detection in (multivariate) observations. R package version 0.1-1 Edition.
URL `http://cran.r-project.org/web/packages/npcp/`

686 Kojadinovic, I., Yan, J., 2010. Modeling multivariate distributions with continu-
687 ous margins using the copula R package. J. Statist. Software 34 (9), 1–20.

688 Koutsoyiannis, D., 2001. Coupling stochastic models of different time scales. Wa-
689 ter Resources Research 37 (2), 379–391.

690 Koutsoyiannis, D., Onof, C., 2001. Rainfall disaggregation using adjusting proce-
691 dures on a Poisson cluster model. Journal of Hydrology 246, 109–122.

692 Laaha, G., Blöschl, G., 2006a. A comparison of low flow regionalisation methods-
693 catchment grouping. Journal of Hydrology 323 (1-4), 193–214.

694 Laaha, G., Blöschl, G., 2006b. Seasonality indices for regionalizing low flows.
695 Hydrological Processes 20 (18), 3851–3878.

696 Larsen, J., Sivapalan, M., Coles, N., Linnet, P., 1994. Similarity analysis of
697 runoff generation processes in real-world catchments. Water Resources Re-
698 search 30 (6), 1641–1652.

699 Louie, H., 2014. Evaluation of bivariate Archimedean and elliptical copulas to
700 model wind power dependency structures. Wind Energy 17 (2), 225–240.

701 McDonnell, J., Woods, R., 2004. On the need for catchment classification. Journal
702 of Hydrology 299 (1-2), 2–3.

703 Merz, R., Blöschl, G., 2005. Flood frequency regionalisation - spatial proximity
704 vs. catchment attributes. Journal of Hydrology 302 (1-4), 283–306.

705 Merz, R., Piock-Ellena, U., Blöschl, G., Gutknecht, D., 1999. Seasonally of flood
706 processes in austria. IAHS-AISH Publication 255, 273–278.

707 Motamedi, M., Liang, R., 2014. Probabilistic landslide hazard assessment using
708 Copula modeling technique. Landslides 11 (4), 565–573.

709 Nelsen, R. B., 2006. An introduction to copulas, 2nd Edition. Springer-Verlag,
710 New York.

711 Onof, C., Wheater, H. S., 1993. Modelling of British rainfall using a Random
712 Parameter Bartlett-Lewis Rectangular Pulse Model. Journal of Hydrology 149,
713 67–95.

714 Onof, C., Wheater, H. S., 1994. Improvements to the modelling of British rainfall
715 using a Random Parameter Bartlett-Lewis Rectangular Pulse Model. Journal of
716 Hydrology 157, 177–195.

717 Pardé, M., 1947. Fleuves et rivières. 2 ed. rev. et corr. Colin, Paris, France.

718 Petersen, T., Devineni, N., Sankarasubramanian, A., 2012. Seasonality of monthly
719 runoff over the continental united states: Causality and relations to mean annual

and mean monthly distributions of moisture and energy. Journal of Hydrology 468-469, 139–150.

Pham, M., Vanhaute, W., Vandenberghe, S., De Baets, B., Verhoest, N., 2013. An assessment of the ability of Bartlett-Lewis type of rainfall models to reproduce drought statistics. Hydrology and Earth System Sciences 17 (12), 5167–5183.

Rémillard, B., Plante, J.-F., 2012. TwoCop: Nonparametric test of equality between two copulas. R package version 1.0 Edition.
URL `http://cran.r-project.org/web/packages/TwoCop/`

Rémillard, B., Scaillet, O., 2009. Testing for equality between two copulas. Journal of Multivariate Analysis 100, 377–386.

Renard, B., Lang, M., 2007. Use of a Gaussian copula for multivariate extreme value analysis: Some case studies in hydrology. Advances in Water Resources 30 (4), 897–912.

Robinson, J., Sivapalan, M., 1997. An investigation into the physical causes of scaling and heterogeneity of regional flood frequency. Water Resources Research 33 (5), 1045–1059.

Salvadori, G., De Michele, C., 2004. Frequency analysis via copulas: theoret-

737 ical aspects and applications to hydrological events. Water Resour. Res. 40,
738 W12511, doi: 10.1029/2004WR003133.

739 Salvadori, G., De Michele, C., 2006. Statistical characterization of temporal
740 structure of storms. Advances in Water Resources 29 (6), 827–842, doi:
741 10.1016/j.advwatres.2005.07.013.

742 Salvadori, G., De Michele, C., 2010. Multivariate multiparameter extreme value
743 models and return periods: A copula approach. Water Resour. Res. 46,
744 W10501, doi: 10.1029/2009WR009040.

745 Salvadori, G., De Michele, C., 2011. Estimating strategies for multiparameter
746 multivariate extreme value copulas. Hydrol. Earth Syst. Sci. 15, 141–150, doi:
747 10.5194/hess-15-141-2011.

748 Salvadori, G., De Michele, C., 2015. Multivariate real-time assessment of
749 droughts via Copula-based multi-site Hazard Trajectories and Fans. Journal of
750 Hydrology 526, 101–115, doi: 10.1016/j.jhydrol.2014.11.056.

751 Salvadori, G., De Michele, C., Durante, F., 2011. On the return period and de-
752 sign in a multivariate framework. Hydrol. Earth Syst. Sci. 15, 3293–3305, doi:
753 10.5194/hess-15-3293-2011.

Salvadori, G., De Michele, C., Kottegoda, N., Rosso, R., 2007. Extremes in Nature. An approach using Copulas. Vol. 56 of Water Science and Technology Library Series. Springer, Dordrecht, iSBN: 978-1-4020-4415-1.

Salvadori, G., Durante, F., De Michele, C., 2013. Multivariate return period calculation via survival functions. Water Resour. Res. 49, 2308–2311.

Salvadori, G., Durante, F., Tomasicchio, G. R., D'Alessandro, F., 2015. Practical guidelines for the multivariate assessment of the structural risk in coastal and off-shore engineering. Coastal Engineering 95, 77–83.

Samaniego, L., Bárdossy, A., Kumar, R., 2010. Streamflow prediction in ungauged catchments using copula-based dissimilarity measures. Water Resources Research 46 (2).

Sawicz, K., Wagener, T., Sivapalan, M., Troch, P., Carrillo, G., 2011. Catchment classification: Empirical analysis of hydrologic similarity based on catchment function in the eastern usa. Hydrology and Earth System Sciences 15 (9), 2895–2911.

Shiau, J.-T., Feng, S., Nadarajah, S., 2007. Assessment of hydrological droughts for the Yellow River, China, using copulas. Hydrological Processes 21 (16), 2157–2163.

772 Sklar, A., 1959. Fonctions de répartition à n dimensions et leurs marges. Publ.
773 Inst. Statist. Univ. Paris 8, 229–231.

774 The European Parliament and The Council, 6.11.2007. Directive 2007/60/EC: on
775 the assessment and management of flood risks. Official Journal of the European
776 Union.

777 USDA-NRCS, 2010. National Engineering Handbook, Part 630 - Hydrology.
778 Tech. rep., United States Department of Agriculture, Natural Resources Con-
779 servation Service.

780 USDA-SCS, 1986. Urban hydrology for small watersheds. Technical release 55,
781 United States Department of Agriculture, Soil Conservation Service, Washing-
782 ton, DC.

783 Vandenberghe, S., Verhoest, N., Onof, C., De Baets, B., 2011. A comparative
784 copula-based bivariate frequency analysis of observed and simulated storm
785 events: A case study on Bartlett-Lewis modeled rainfall. Water Resources Re-
786 search 47 (7).

787 Volpi, E., Fiori, A., 2014. Hydraulic structures subject to bivariate hydrological
788 loads: Return period, design, and risk assessment. Water Resources Research
789 50 (2), 885–897.

790 Ye, S., Yaeger, M., Coopersmith, E., Cheng, L., Sivapalan, M., 2012. Exploring
791 the physical controls of regional patterns of flow duration curves part 2: Role of
792 seasonality, the regime curve, and associated process controls. Hydrology and
793 Earth System Sciences 16 (11), 4447–4465.

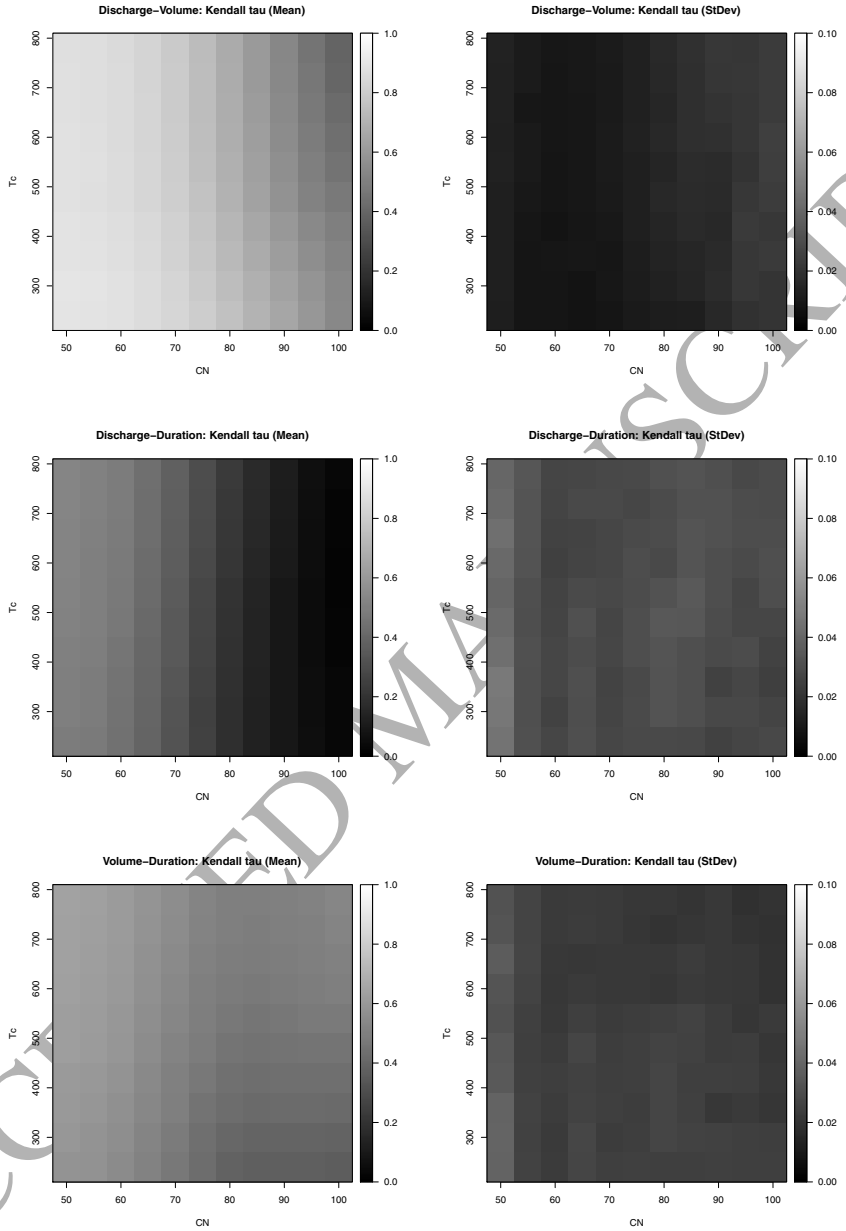

Figure 1: Estimates of the Kendall τ, over all the available N_S series, for different BS's and variables — see text: (*left* column) sample average; (*right* column) sample standard deviation.

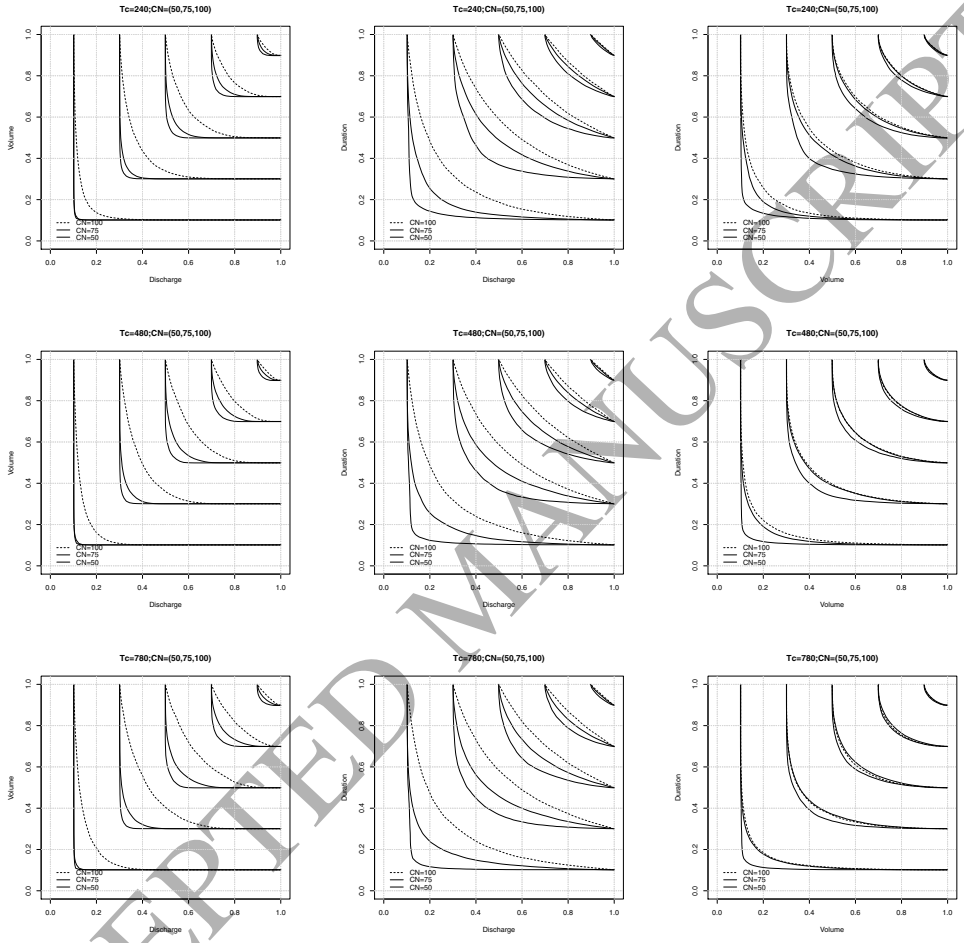

Figure 2: Comparison of the (average) Empirical Copulas, for fixed T_c's (*rows*) and different *CN*'s — see text: (*left* column) the Discharge-Volume pair, (*middle* column) the Discharge-Duration pair, and (*right* column) the Volume-Duration pair.

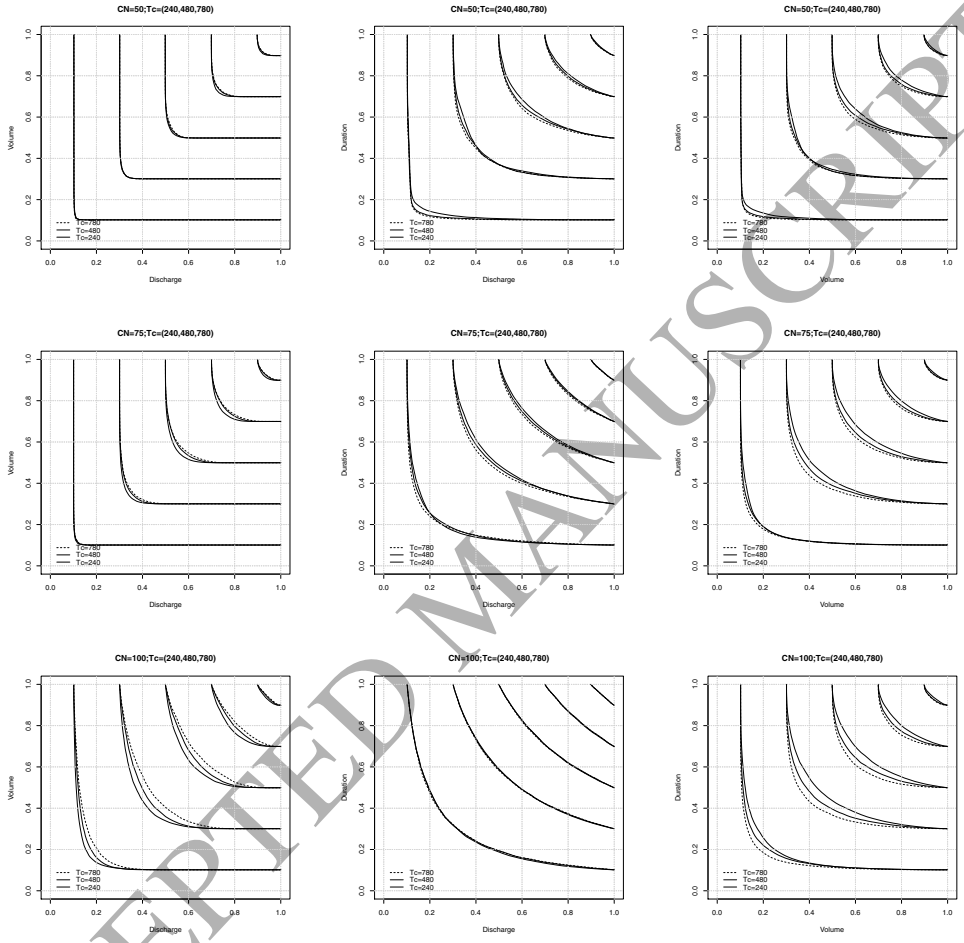

Figure 3: Comparison of the (average) Empirical Copulas, for fixed *CN*'s (*rows*) and different T_c's — see text: (*left* column) the Discharge-Volume pair, (*middle* column) the Discharge-Duration pair, and (*right* column) the Volume-Duration pair.

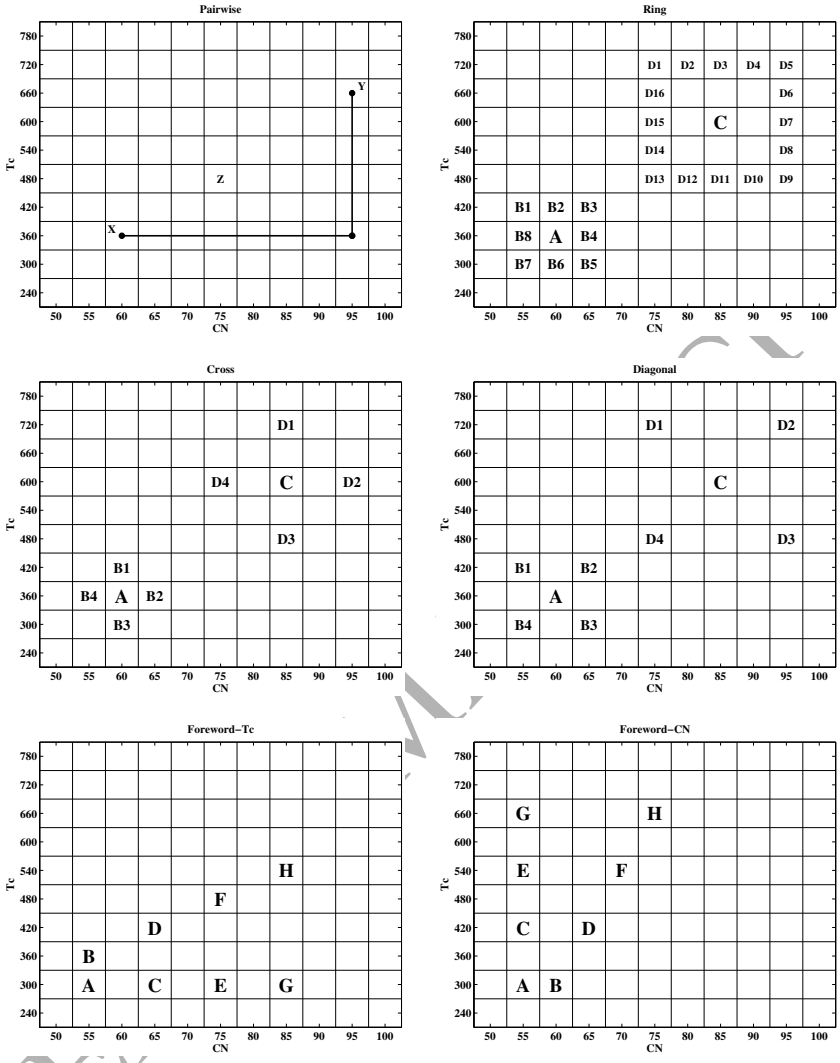

Figure 4: Illustration of the strategies for investigating the compatibility of Basin Scenario outlined in Section 3.4. (*Top-left*) Pairwise. (*Top-right*) Ring. (*Middle-left*) Cross. (*Middle-right*) Diagonal. (*Bottom-left*) Foreword-T_c. (*Bottom-right*) Foreword-CN. Four different d's are shown: respectively, $d = 1$ (A and B's pairs), $d = 2$ (C and D's pairs), $d = 3$ (E and F's pairs), and $d = 4$ (G and H's pairs). In the *Top-left* panel is also indicated the "central" BS Z considered in Section 3.4.

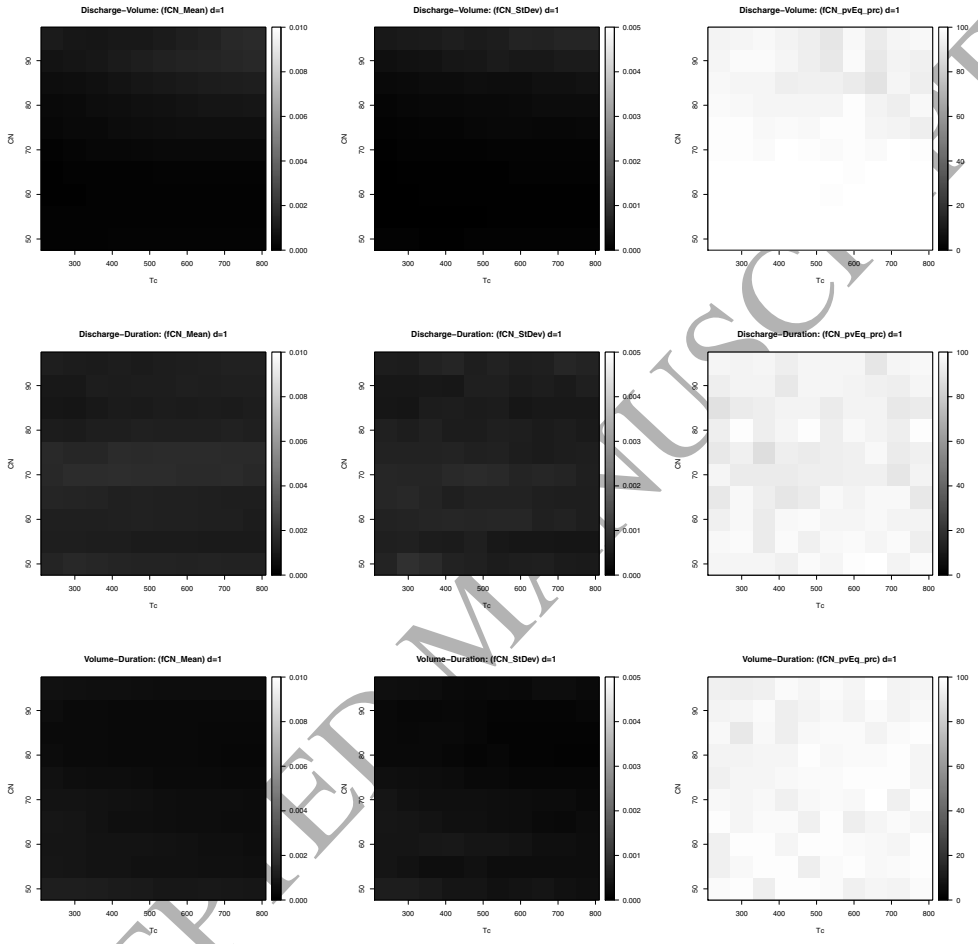

Figure 5: Values of the Foreword-*CN* distances, over all the available N_S series, for different BS's and variables, using $d = 1$ — see text: (*left* column) sample average; (*middle* column) sample standard deviation. The *right* column shows the corresponding CM's: indicated are the percentages of non-rejection of $\mathcal{H}_0$.

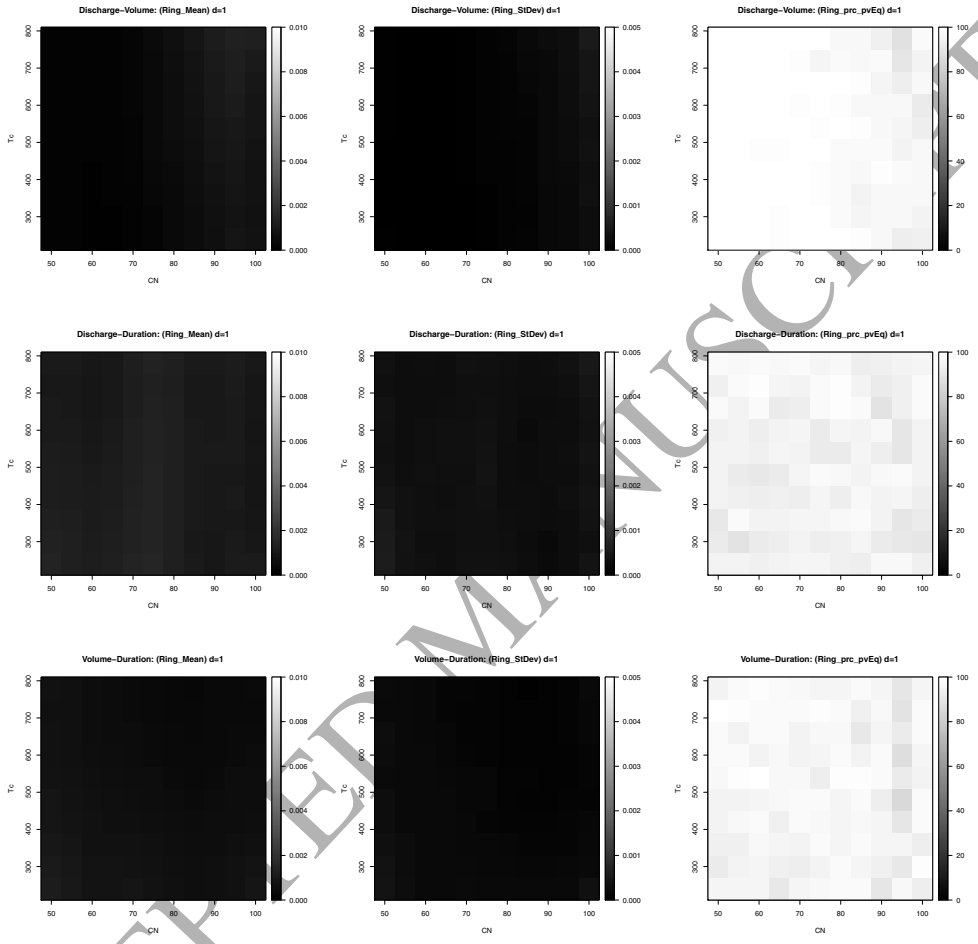

Figure 6: Values of the Ring distances, over all the available N_S series, for different BS's and variables, using $d = 1$ — see text: (*left* column) sample average; (*middle* column) sample standard deviation. The *right* column shows the corresponding CM's: indicated are the percentages of non-rejection of $\mathcal{H}_0$.

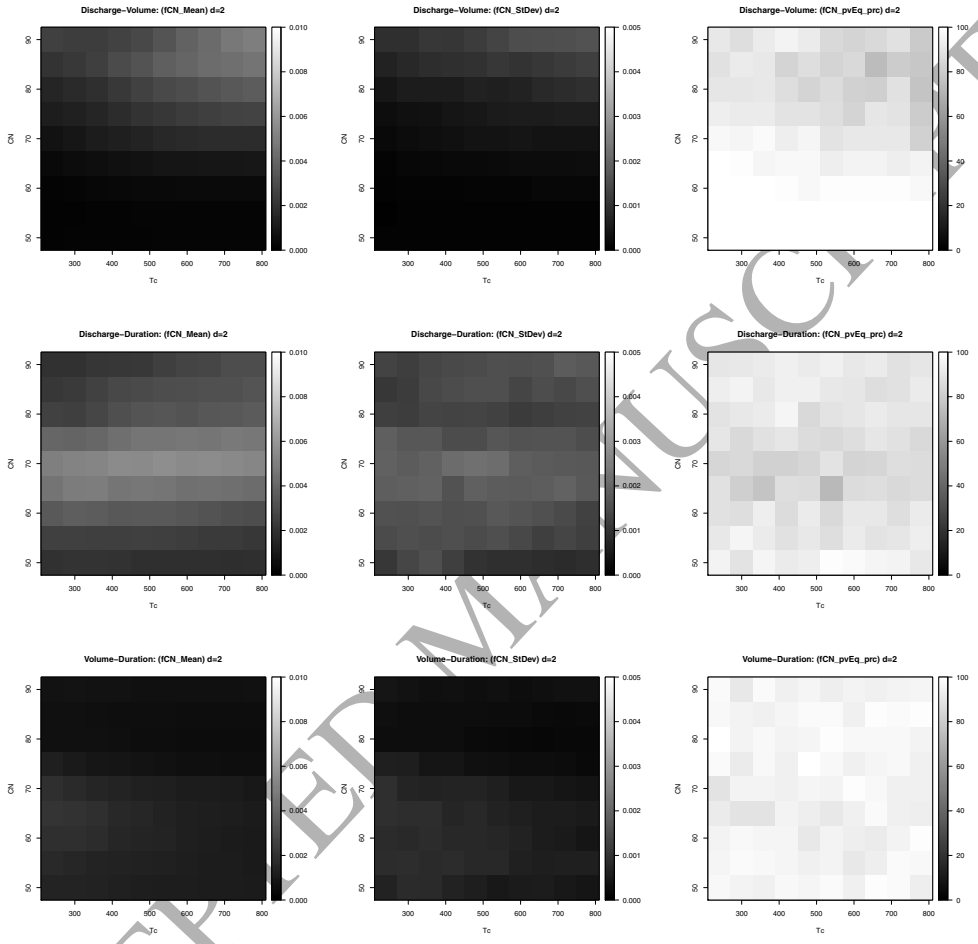

Figure 7: Values of the Foreword-CN distances, over all the available N_S series, for different BS's and variables, using $d = 2$ — see text: (*left* column) sample average; (*middle* column) sample standard deviation. The *right* column shows the corresponding CM's: indicated are the percentages of non-rejection of $\mathcal{H}_0$.

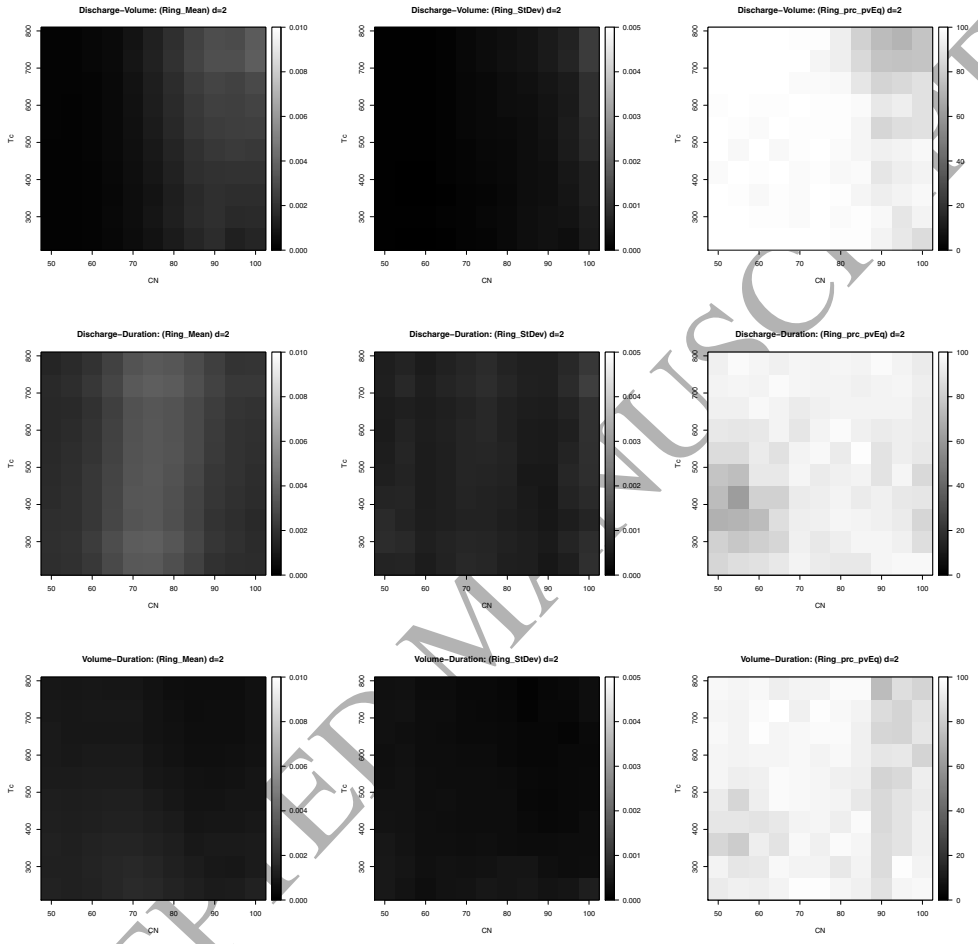

Figure 8: Values of the Ring distances, over all the available N_S series, for different BS's and variables, using $d = 2$ — see text: (*left* column) sample average; (*middle* column) sample standard deviation. The *right* column shows the corresponding CM's: indicated are the percentages of non-rejection of $\mathcal{H}_0$.

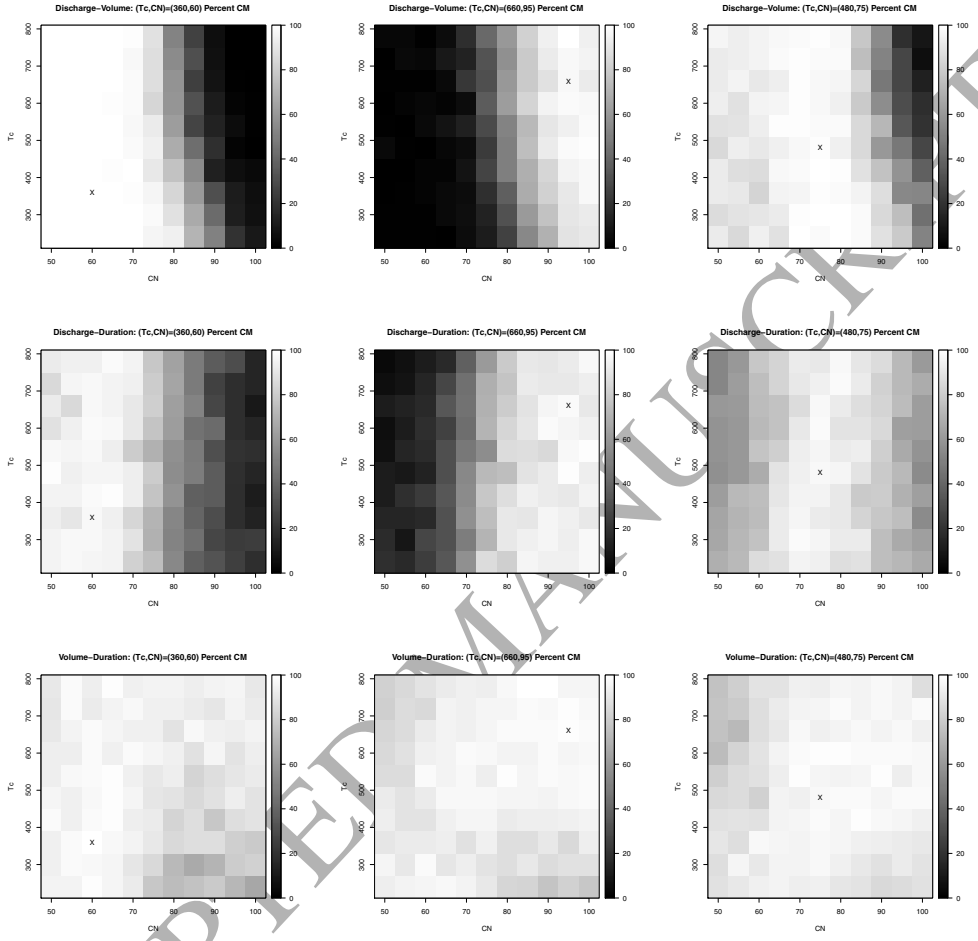

Figure 9: Pairwise Compatibility Maps, for the three BS's labelled X, Y, and Z in Figure 4(top-left), for different variables — see text: the reference BS is marked as "x". (*Left* column) CM's for the BS X ($T_c = 360, CN = 60$). (*Middle* column) CM's for the BS Y ($T_c = 660, CN = 95$). (*Right* column) CM's for the BS Z ($T_c = 480, CN = 75$). The colormap indicates the percentages of non-rejection of $\mathcal{H}_0$.

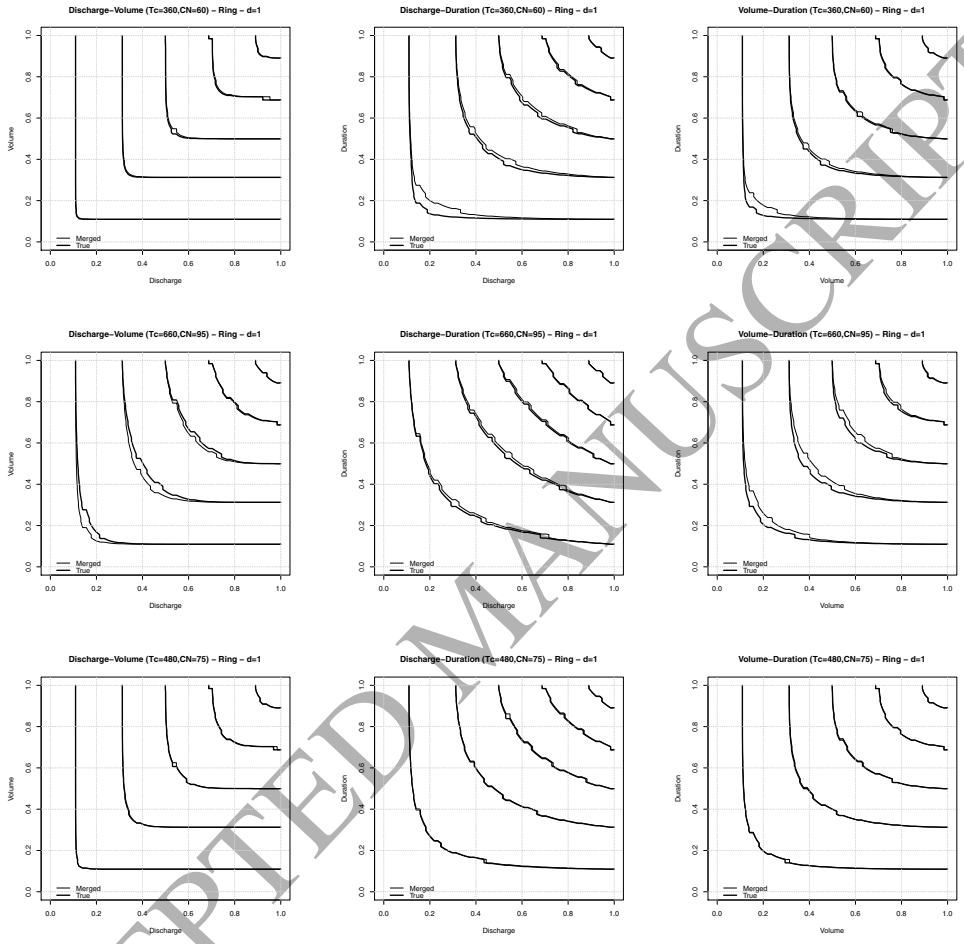

Figure 10: Comparison between the (average) Empirical Copulas of the "true" and the "merged" series, for $d = 1$, considering the BS's X (*top* row), Y (*middle* row), and Z (*bottom* row) — see text: (*left* column) the Discharge-Volume pair, (*middle* column) the Discharge-Duration pair, and (*right* column) the Volume-Duration pair.

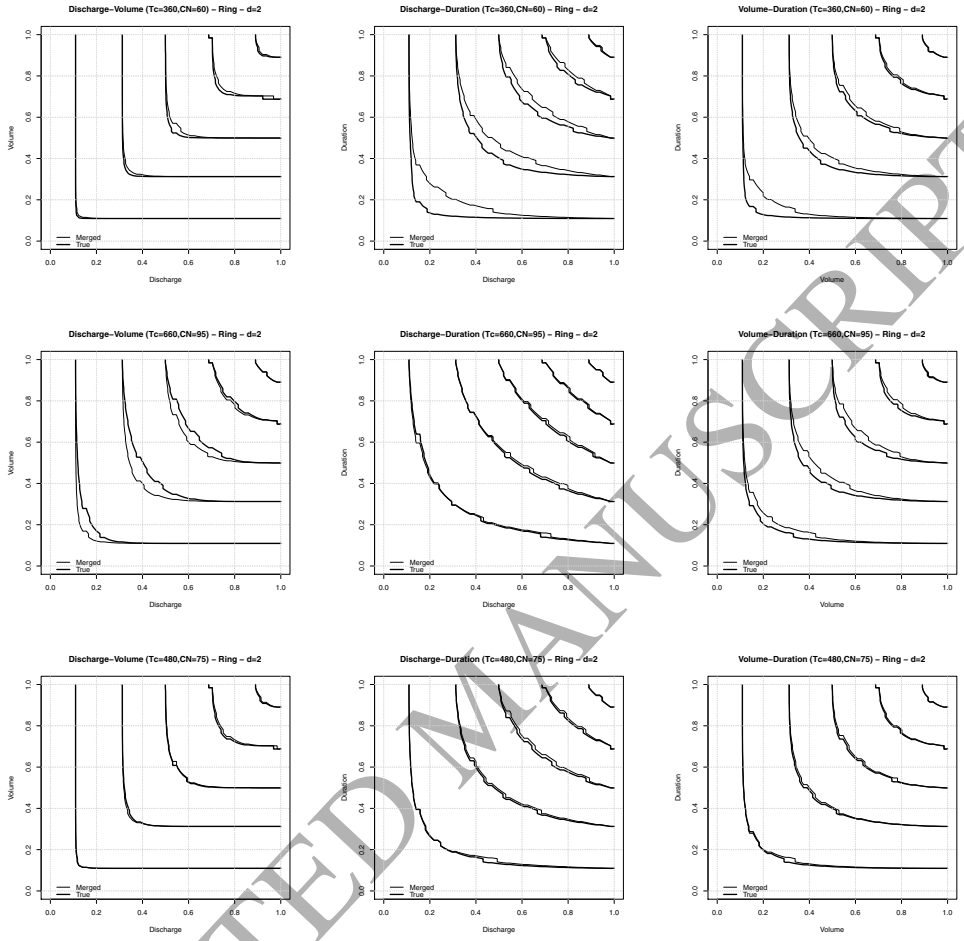

Figure 11: Same as Figure 10, for $d = 2$.

Table 1: The main features of the Torbido watershed case study — see text.

DEM source	IGMI
Cell size (m)	20
Precision	integer
Outlet coordinate North - UTM 33 N	4721505
Outlet coordinate East - UTM 33 N	272623
Area (Km^2)	61.67
Min elevation (m)	85.0
Max elevation (m)	625.0
Mean elevation (m)	373.8
Max slope (%)	375.0
Mean slope (%)	21.9
Main channel length (Km)	24.50
Maximum divide-outlet distance (Km)	25.81

Table 2: Sample averages and standard deviations (in parentheses) of the distance δ, for the pairs of BS's {X,Y}, {X,Z}, and {Y,Z}, considering the variables Discharge-Volume, Discharge-Duration, and Volume-Duration — see text.

Pair	**Dis.-Vol.**	**Dis.-Dur.**	**Vol.-Dur.**
(X,Y)	0.0204	0.0332	0.0023
	(0.0030)	(0,0067)	(0.0009)
(X,Z)	0.0013	0.0075	0.0023
	(0.0004)	(0.0031)	(0.0012)
(Y,Z)	0.0129	0.0113	0.0010
	(0.0022)	(0.0035)	(0.0005)

Table 3: Percentages of non-rejection of $\mathcal{H}_0$ under the Ring strategy, for $d = 1$, considering the pairs Discharge-Volume, Discharge-Duration, and Volume-Duration — see text.

BS	(T_c, CN)	**Dis.-Vol.**	**Dis.-Dur.**	**Vol.-Dur.**
X	$(360, 60)$	99.93	94.17	95.97
Y	$(660, 95)$	92.70	94.10	91.80
Z	$(480, 75)$	99.33	95.73	96.47

Table 4: Same as Table 3, for $d = 2$.

BS	(T_c, CN)	**Dis.-Vol.**	**Dis.-Dur.**	**Vol.-Dur.**
X	$(360, 60)$	98.63	74.03	87.10
Y	$(660, 95)$	83.47	94.13	87.43
Z	$(480, 75)$	99.03	94.87	95.33

Appendix A. More compatibility criteria

In addition to the compatibility criteria illustrated in Section 3.4, the following three strategies can also be considered.

1. The Foreword-T_c BS (individual) distance of size d is defined as the average δ distance (over the N_s series) between the BS's $\mathcal{S}_1 = (T_c, CN)$ and $\mathcal{S}_2 = (T_c + d \cdot \Delta_{T_c}, CN)$. The notion is illustrated in Figure 4(bottom-left), using d's ranging from 1 to 4. A corresponding Foreword-T_c BS compatibility can be introduced.
2. The Cross BS (ensemble) distance of size d is defined as the average (over the N_s series) of the average δ distance between the BS $\mathcal{S} = (T_c, CN)$ and the neighboring BS's $(T_c \pm d \cdot \Delta_{T_c}, CN)$ and $(T_c, CN \pm d \cdot \Delta_{CN})$. The notion is illustrated in Figure 4(middle-left), for d equal to 1 and 2. Practically, the Cross distance is the average of the BS distances considering only the neighbors of $\mathcal{S}$ positioned on a suitable "cross" on the T_c–CN grid. Note that, each of the neighbor BS's have only one of the parameters CN or T_c different from the reference BS $\mathcal{S}$: this corresponds to average over "partial" changes of the basin parameters. A corresponding Cross BS compatibility can be introduced.
3. The Diagonal BS (ensemble) distance of size d is defined as the average

(over the N_s series) of the average δ distance between the BS $\mathcal{S} = (T_c, CN)$ and the neighboring BS's $(T_c \pm d \cdot \Delta_{T_c}, CN \pm d \cdot \Delta_{CN})$. The notion is illustrated in Figure 4(middle-right), for d equal to 1 and 2. Practically, the Diagonal distance is the average of the BS distances considering only the neighbors of $\mathcal{S}$ positioned on a suitable "crux decussata" (Saint Andrew's Cross) on the T_c–CN grid. Note that, each of the neighbor BS's have both of the parameters CN and T_c different from the reference BS $\mathcal{S}$: this corresponds to average over "total" changes of the basin parameters. A corresponding Diagonal BS compatibility can be introduced.

Practically, the Foreword-T_c approach is a special case of the Pairwise one, while the Cross and Diagonal strategies are sub-cases of the Ring one.

Appendix B. KS distance of copulas

Let $\mathbf{C}_1$ and $\mathbf{C}_2$ be the copulas associated with, respectively, the BS's $\mathcal{S}_1 = (T_{c,1}, CN_1)$ and $\mathcal{S}_2 = (T_{c,2}, CN_2)$, and denote by $\delta_{1,2}$ the distance between $\mathbf{C}_1$ and $\mathbf{C}_2$. Then, adopting a Kolmogorov-Smirnov (KS) approach, the following definition may be introduced:

$$\delta_{1,2} = 2 \cdot \sup_{\mathbf{u} \in \mathbf{S}} |\mathbf{C}_1(\mathbf{u}) - \mathbf{C}_2(\mathbf{u})| \,, \tag{B.1}$$

where the coefficient "2" is used to normalize δ into the interval $[0, 1]$ (Nelsen, 2006). A consistent empirical estimator $\widetilde{\delta}_{1,2}$ of $\delta_{1,2}$ is given by

$$\widetilde{\delta}_{1,2} = 2 \cdot \max_{\mathbf{u} \in \mathcal{G}} \left| \widetilde{\mathbf{C}}_1(\mathbf{u}) - \widetilde{\mathbf{C}}_2(\mathbf{u}) \right|. \tag{B.2}$$